

Fluorescent Biological Aerosol Particle Measurements at a Tropical High Altitude Site in Southern India: Characteristic properties during Southwest Monsoon Season

A. E. Valsan^{1,*}, R. Ravikrishna², C. V. Biju³, C. Pöhlker⁴, V. R. Després⁵, J. A. Huffman⁶, U. Pöschl⁷, and S. S. Gunthe^{1,**}

¹EWRE Division, Department of Civil Engineering, Indian Institute of Technology Madras, Chennai – 600 036, India.

²Department of Chemical Engineering, Indian Institute of Technology Madras, Chennai – 600 036, India.

³Department of Civil Engineering, College of Engineering Munnar, PB.No:45, County Hills, Munnar – 685612, India.

⁴Biogeochemistry Department, Max Planck Institute for Chemistry, P. O. Box Number 3060, Mainz, Germany.

⁵Institute of General Botany, Johannes Gutenberg University, Mainz, Germany.

⁶Department of Chemistry and Biochemistry, University of Denver, 2190 E. Iliff Ave., Denver, CO, 80208, USA.

⁷Multiphase Chemistry Department, Max Planck Institute for Chemistry, P. O. Box 3060, Mainz, Germany

To whom correspondence should be addressed:

* Aswathy E. Valsan (aswathyerat@gmail.com)

** Sachin S. Gunthe (s.gunthe@iitm.ac.in)



Fig S1: UV-APS inlet

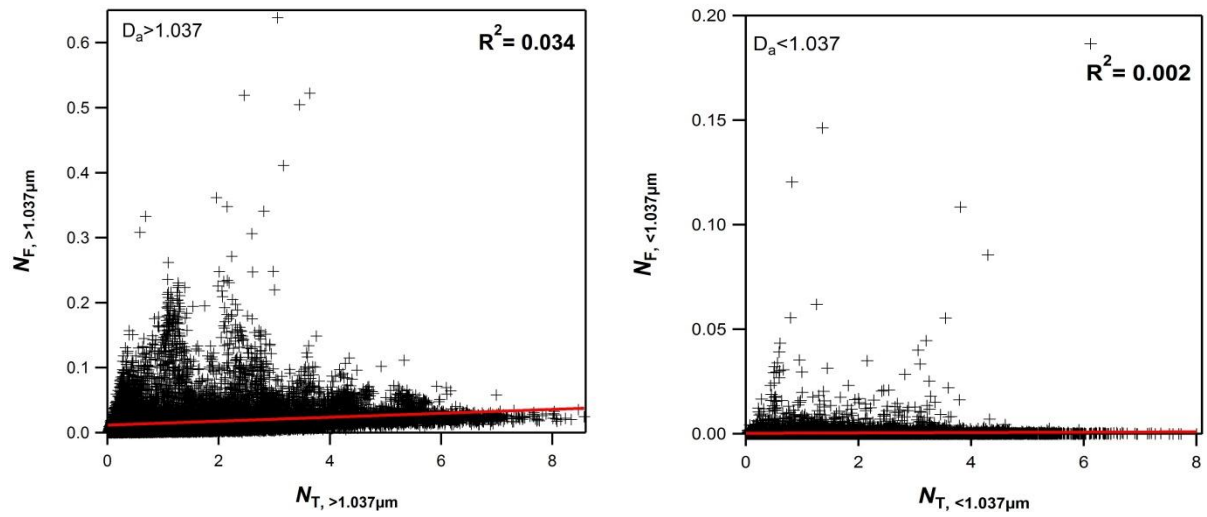


Fig S2: Scatter plots of N_F vs. N_T for particle diameters above (a) and below (b) 1.0 μm , respectively for the entire campaign. $N_{F, < 1.037}$ particle number exhibiting fluorescence in the fine particle mode ($< 1.0 \mu\text{m}$) and $N_{T, < 1.037}$ all particles in size mode. $N_{F, > 1.037}$ and $N_{T, > 1.037}$, represent coarse mode ($> 1.0 \mu\text{m}$).

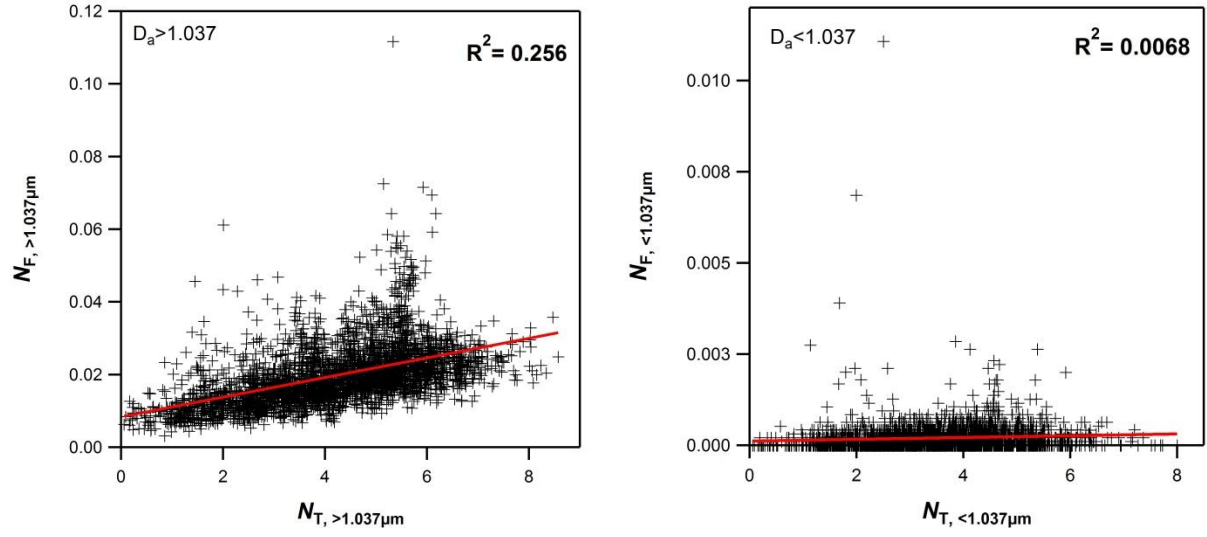
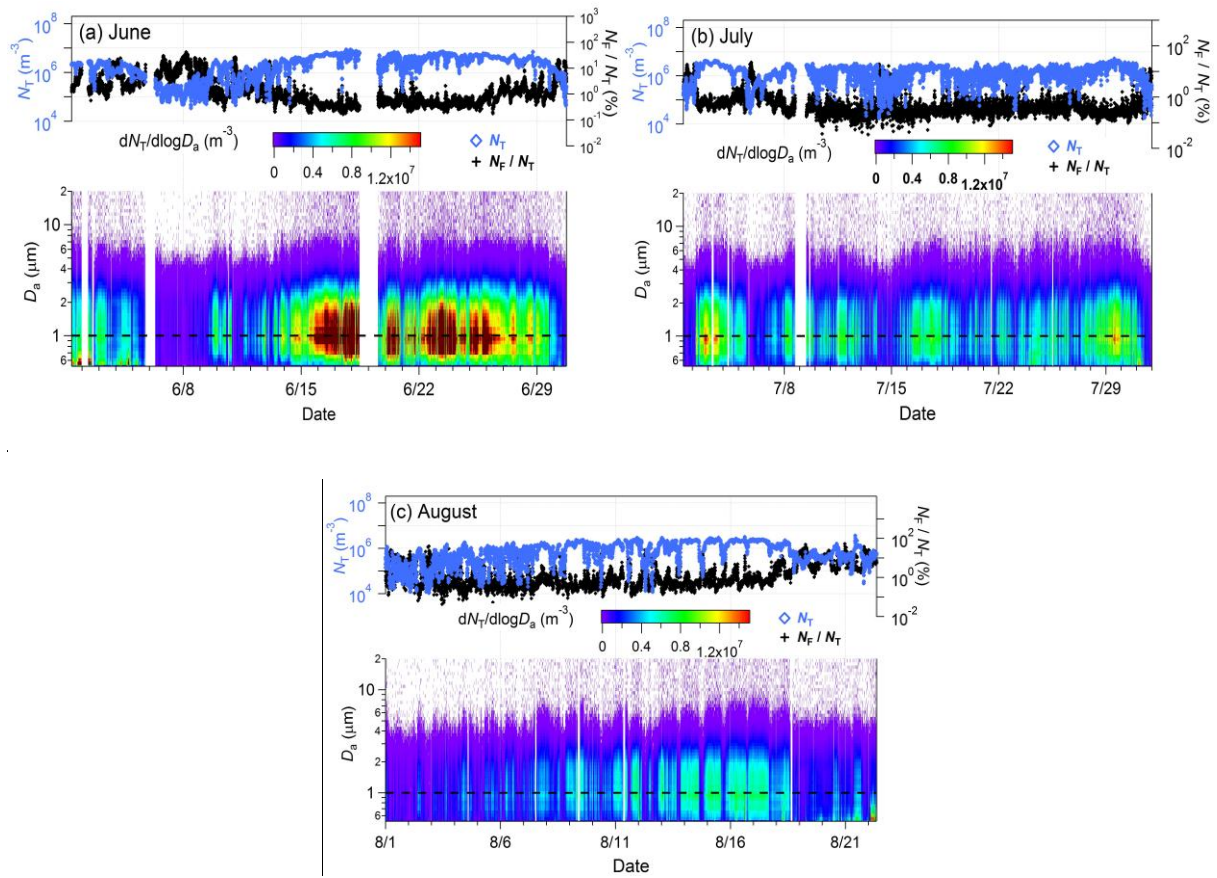
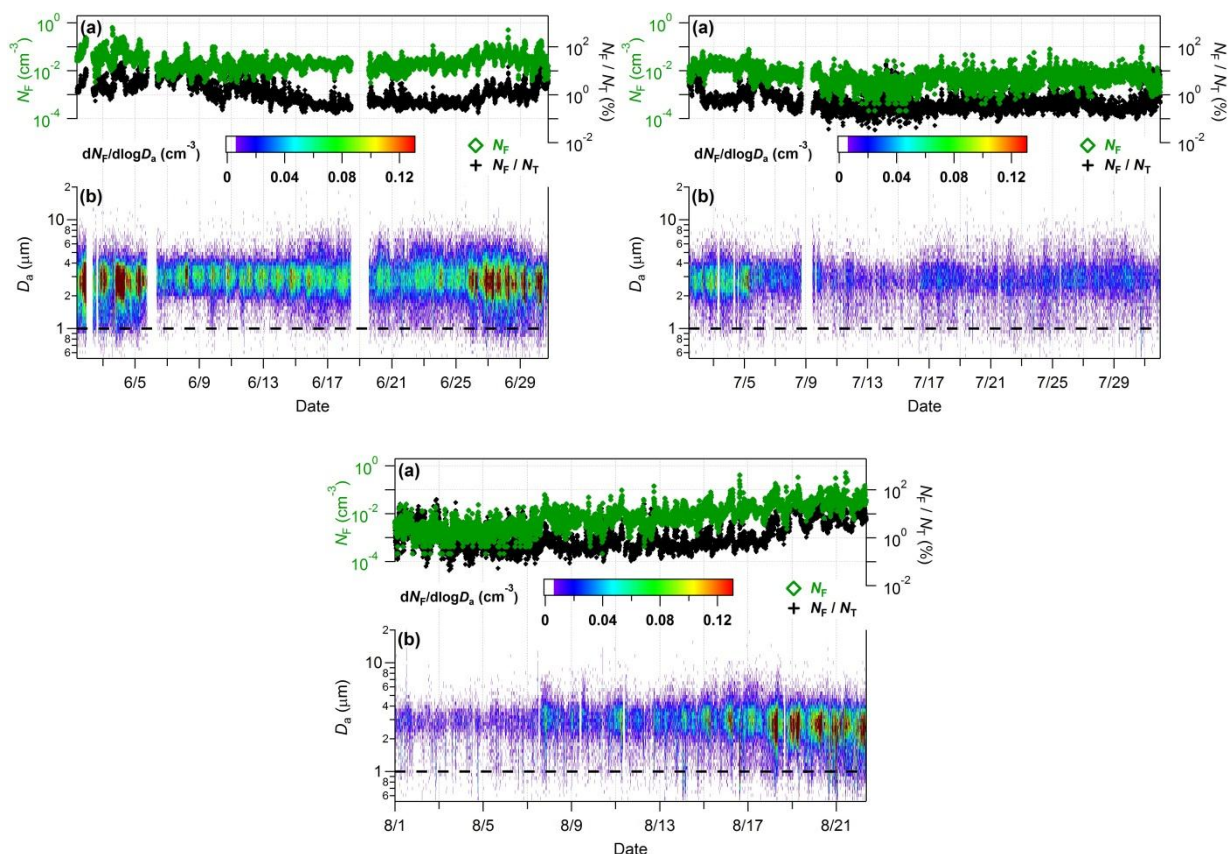


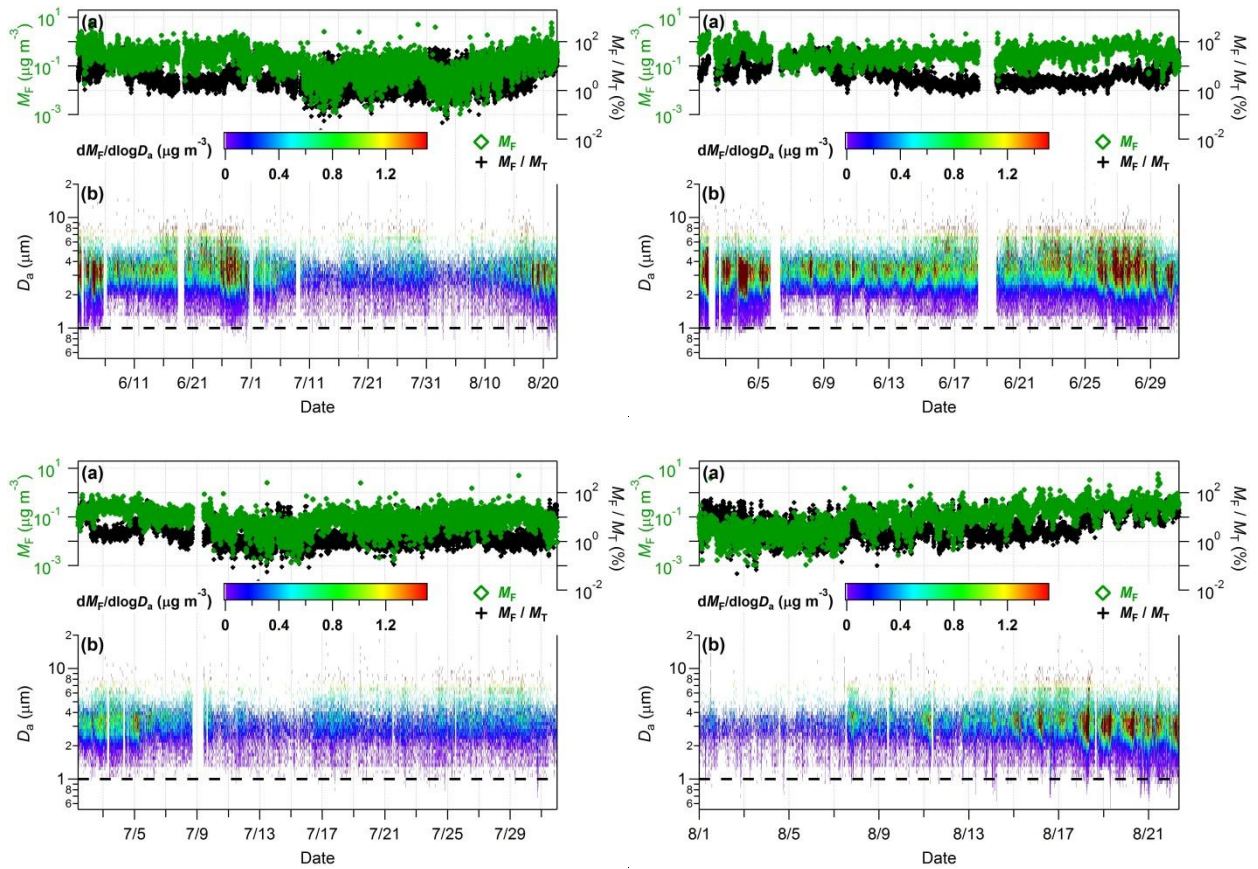
Fig S3: Scatter plots of N_F vs. N_T for particle diameters above (a) and below (b) 1.0 μm , respectively during dusty period. $N_{F, < 1.037}$ particle number exhibiting fluorescence in the fine particle mode ($< 1.0 \mu\text{m}$) and $N_{T, < 1.037}$ all particles in size mode. $N_{F, > 1.037}$ and $N_{T, > 1.037}$, represent coarse mode ($> 1.0 \mu\text{m}$).



S4: Time series of total particle concentration (blue) and ratio of fluorescent to total particles (black) along with size resolved measurements (lower panel) for each individual months (Jun-Aug)



S5: Time series of fluorescent particle concentration (green) and ratio of fluorescent to total particles (black) along with size resolved measurements (lower panel) for each individual months (Jun-Aug). Dashed black lines in lower portion of the each panel at $1.0 \mu\text{m}$ shows the particle size cut-off diameter below which fluorescent particles were not considered as FBAP due to potential interference with non-biological aerosol particles.



S6: Time series of fluorescent particle concentration (green) and ratio of fluorescent to total particles (black) along with size resolved measurements (lower panel) for each individual months (Jun-Aug).

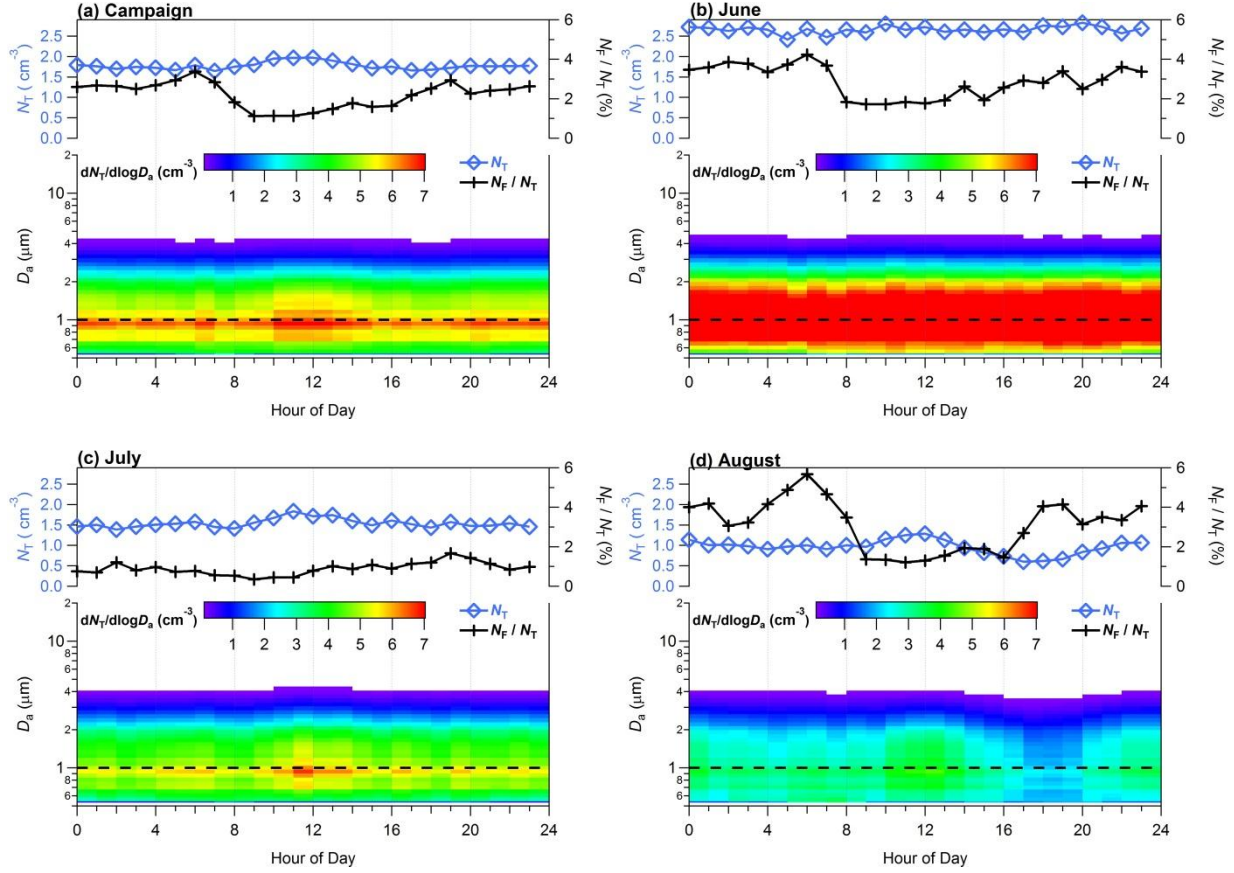
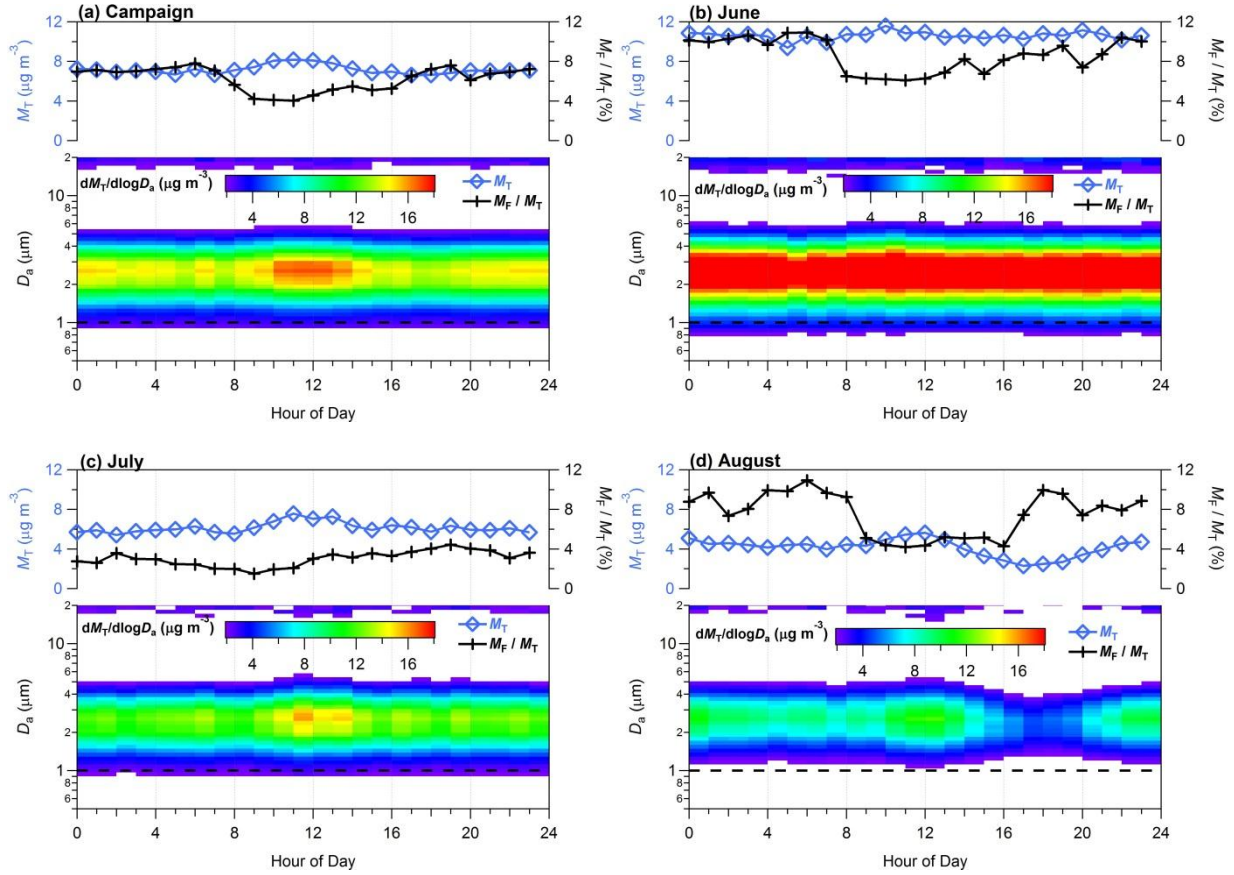


Fig S7: Diurnal cycles of TAP number concentrations (N_T) and size distributions averaged over individual month of measurement and entire campaign (hourly median values plotted against the local time of the day). Upper portion of each panel shows integrated TAP number concentration ($\sim 1 - 20 \mu\text{m}$; N_T) on the left axis (blue color) and FBAP fraction of TAP number (N_F/N_T) on the right axis (black color). Lower portion of each panel TAP number size distribution (3-D plot) plotted against hour of the day on x-axis, aerodynamic diameter on y-axis and color is scaled for $dN_T/d\log D_a$ indicates the concentration. (a) Averaged over entire campaign, (b) Jun, (c) Jul, and (d) Aug.



S8. Diurnal cycles of TAP mass concentrations (N_F) and size distributions averaged over individual month of measurement and entire campaign. Upper portion of each panel shows integrated TAP mass concentration ($\sim 1 - 20 \mu\text{m}$; M_T) on the left axis (blue color) and FBAP fraction of TAP mass (M_F / M_T) on the right axis (black color). Lower portion of each panel FBAP number size distribution (3-D plot) plotted against hour of the day on x-axis, aerodynamic diameter on y-axis and color is scaled for $dM_F / d\log D_a$ indicates the concentration.

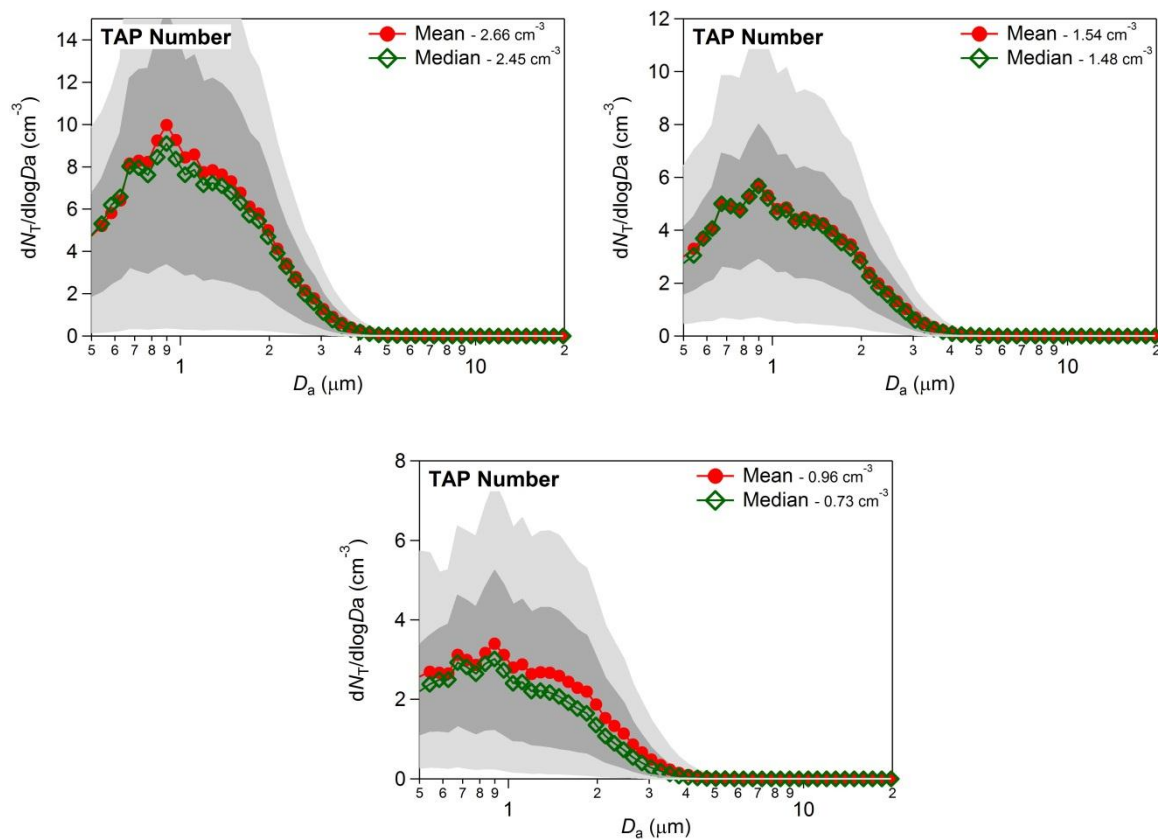


Fig S9: Unit-normalized TAP number size distribution averaged over the individual months (a) June, (b) July, and (c) August during the campaign.

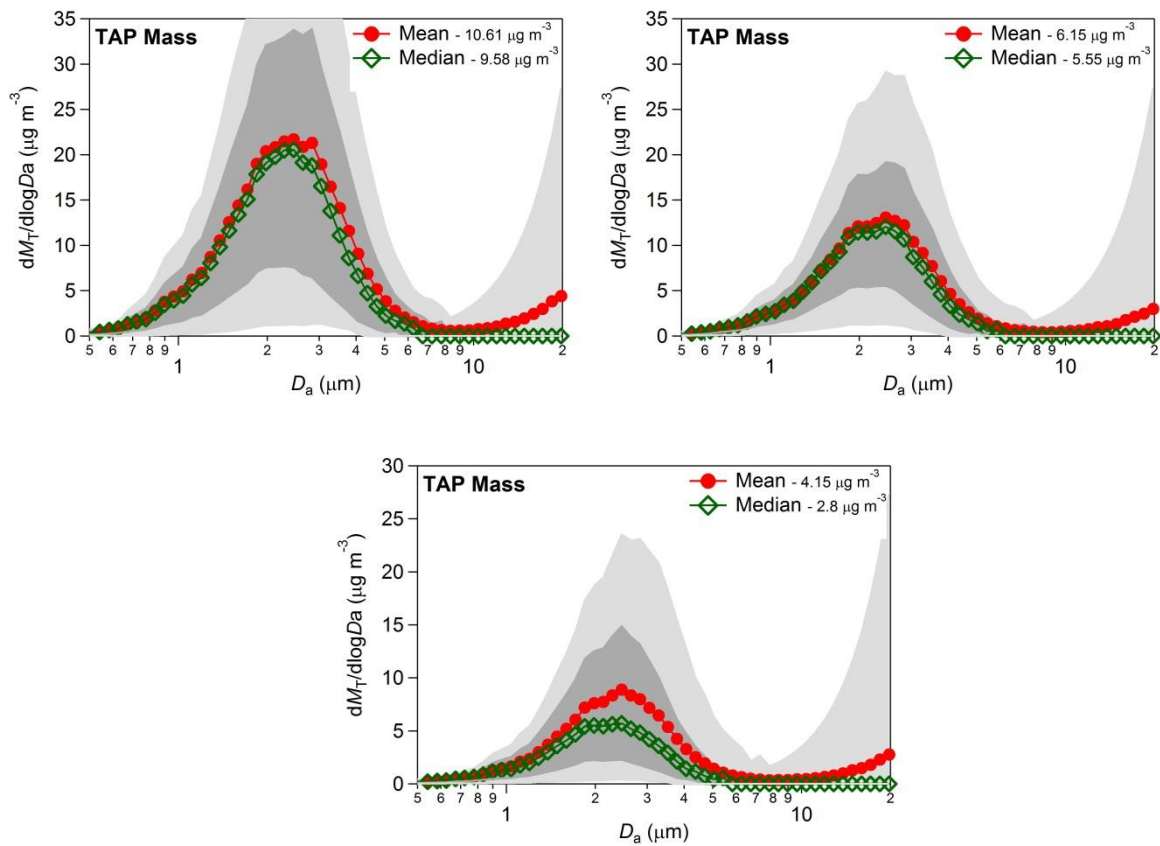


Fig S10: Unit-normalized TAP number size distribution averaged over the individual months (a) June, (b) July, and (c) August during the campaign.

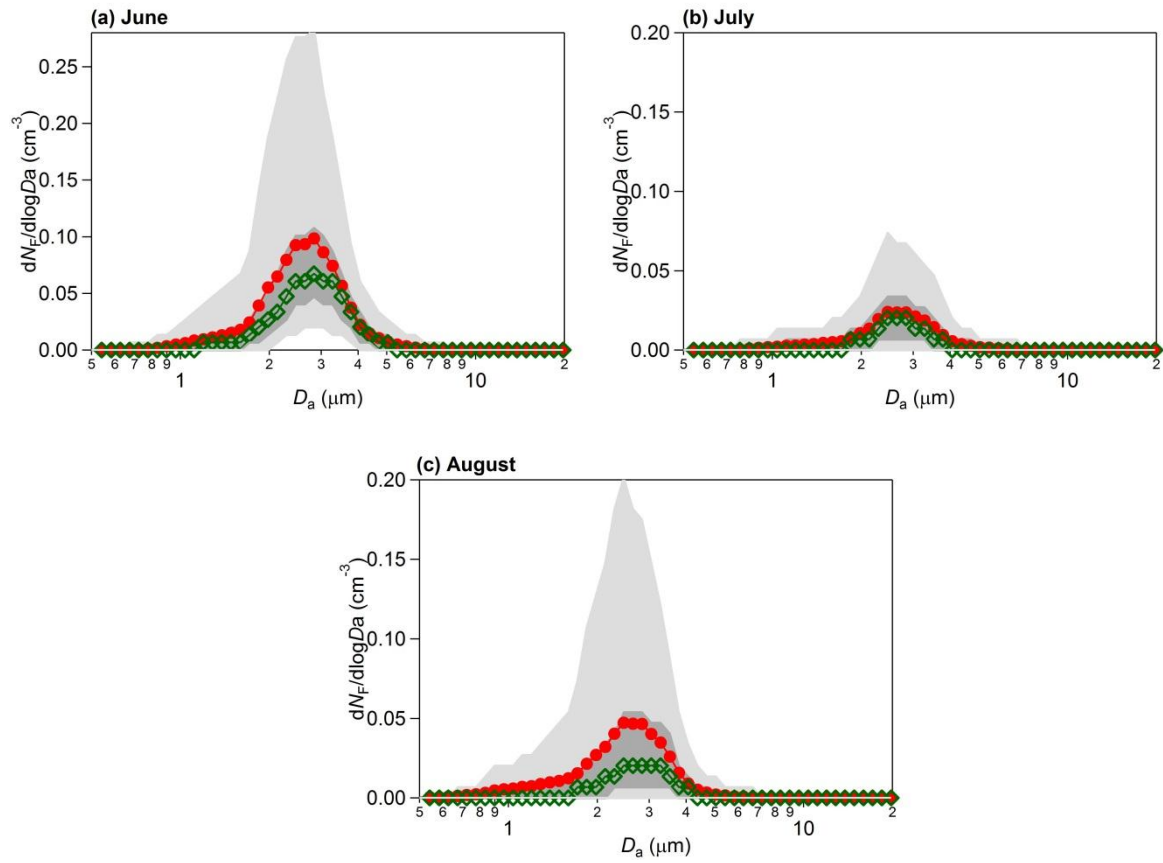


Fig S11: Same as Fig. 7b but representing only FBAP number ($dN_F/d\log D_a$) averaged over individual months (a) Jun, (b) Jul, and (d) Aug.

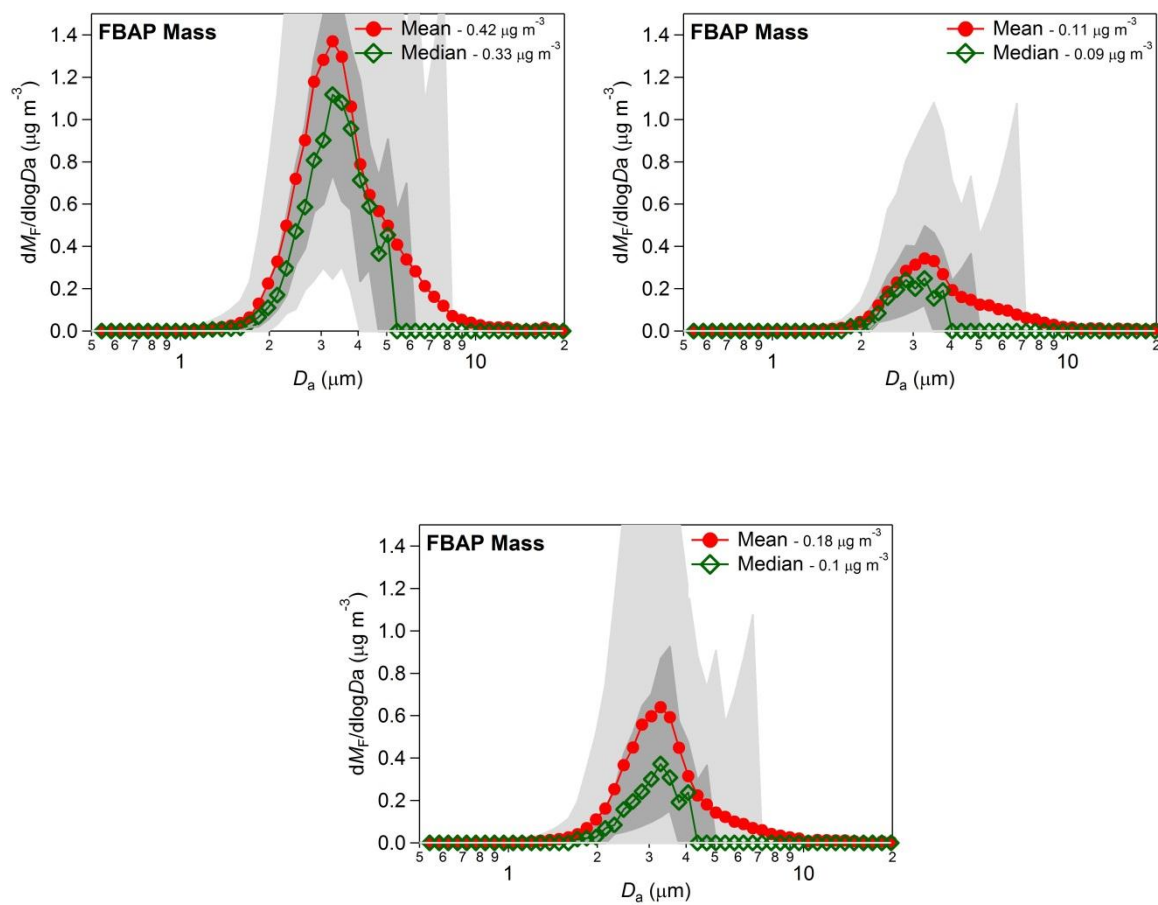


Fig. S12: Same as Fig. S11 but representing FBAP mass ($dM_F/d\log D_a$).

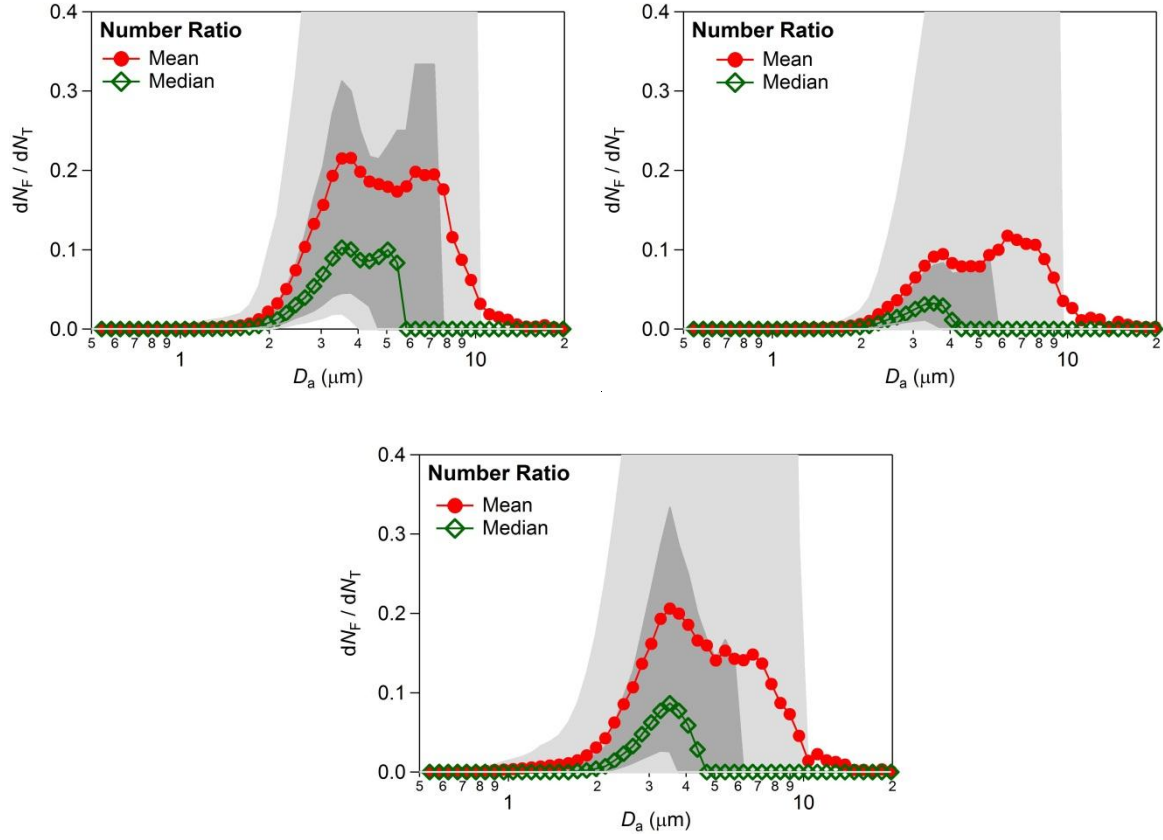


Fig S13: Size distribution of FBAP to TAP ratio averaged over each individual months (Jun-Aug) during the measurements carried out at Munnar ($dN_F/d\log D_a = dM_F/d\log D_a$).

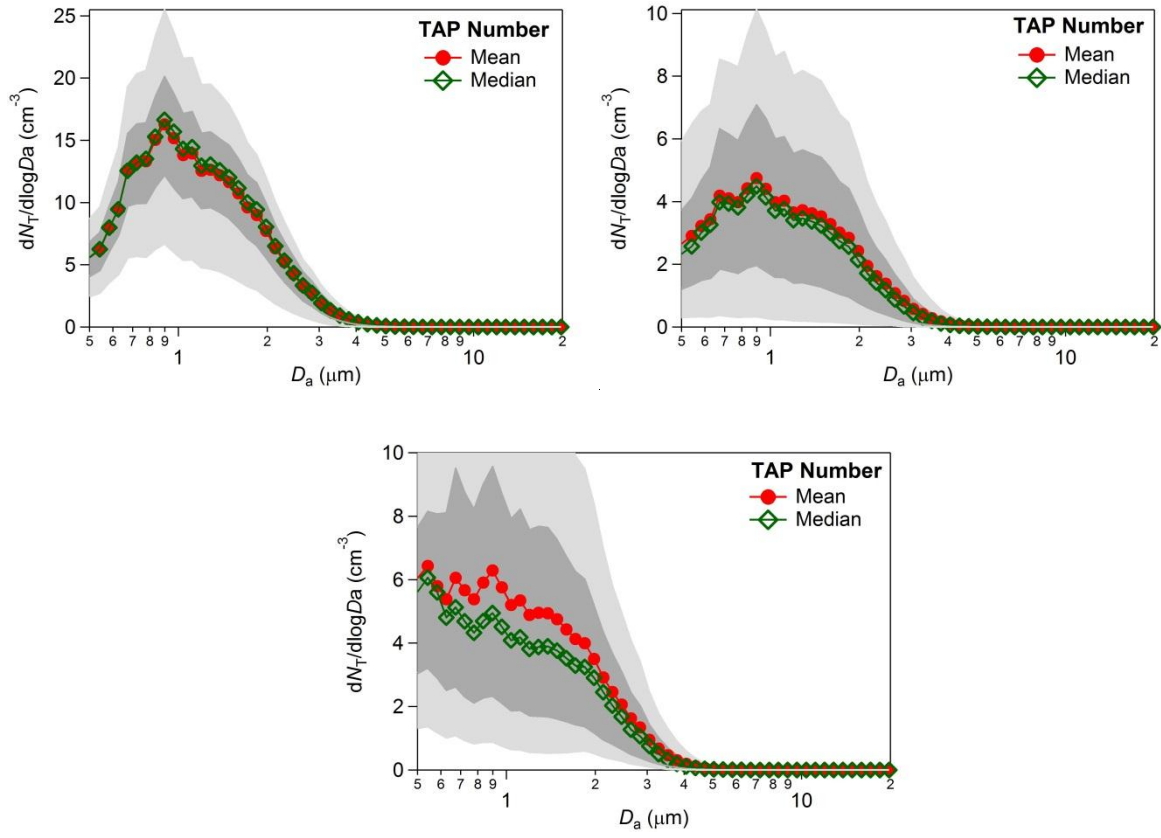


Fig S14: Unit-normalized TAP number size distribution averaged over the each distinct focus periods during the measurements carried out at Munnar.

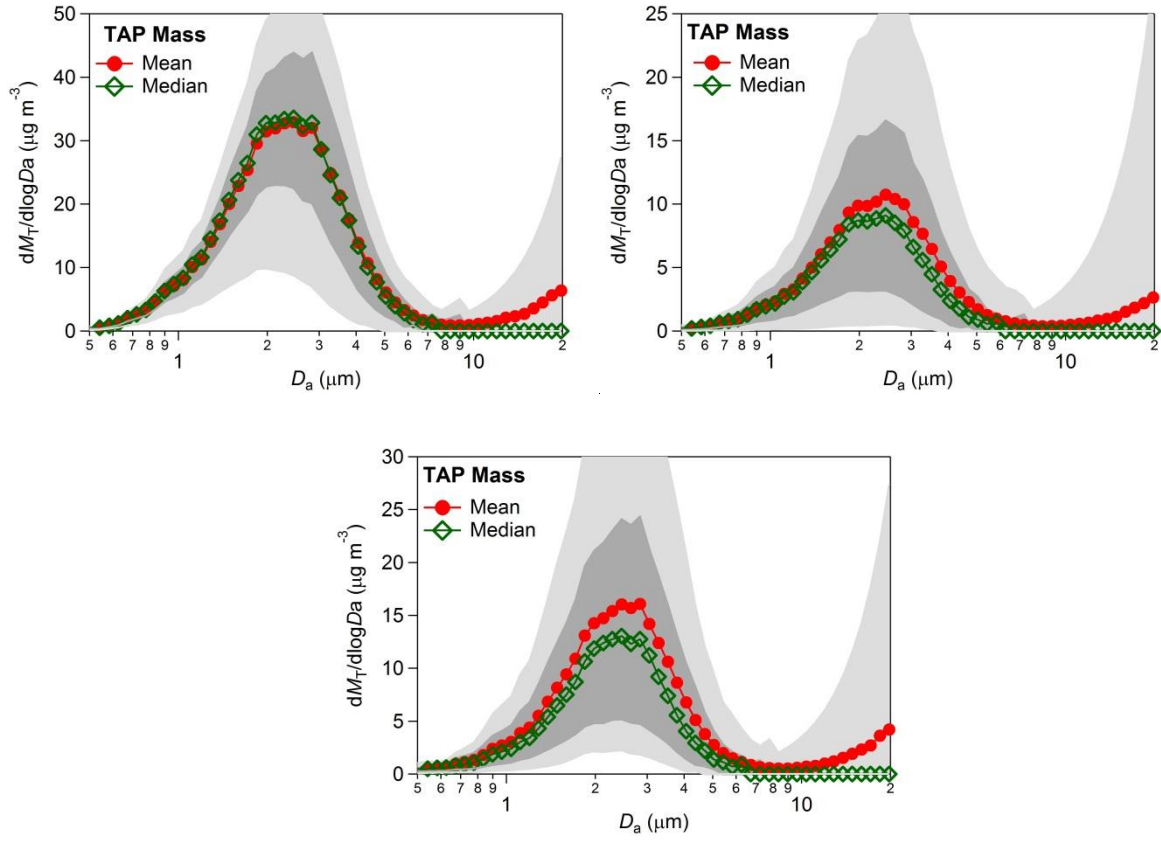


Fig S15: TAP mass size distribution averaged over the each distinct focus periods during the measurements carried out at Munnar.

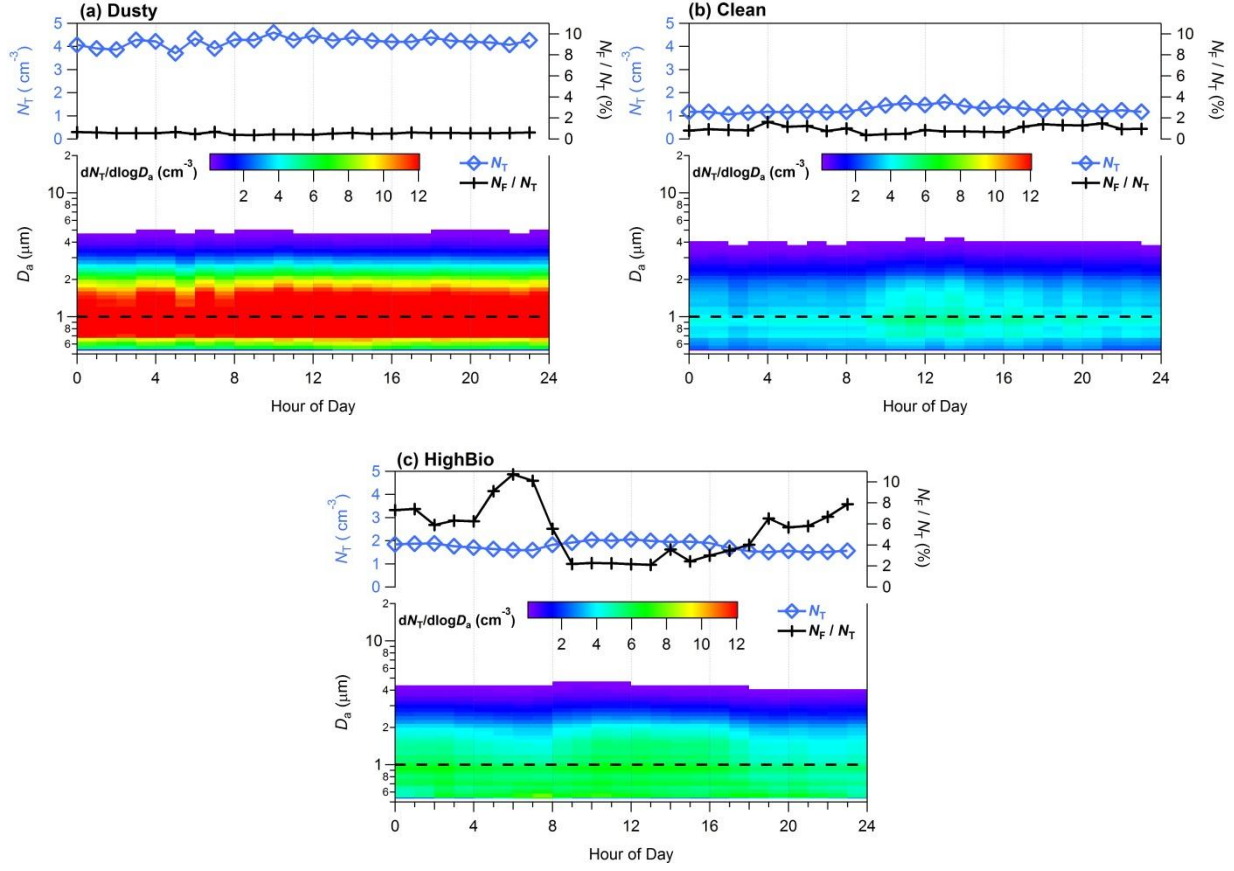


Fig S16: Diurnal cycles of TAP number concentrations (N_T) and size distributions averaged over each distinct focus periods (hourly median values plotted against the local time of the day).

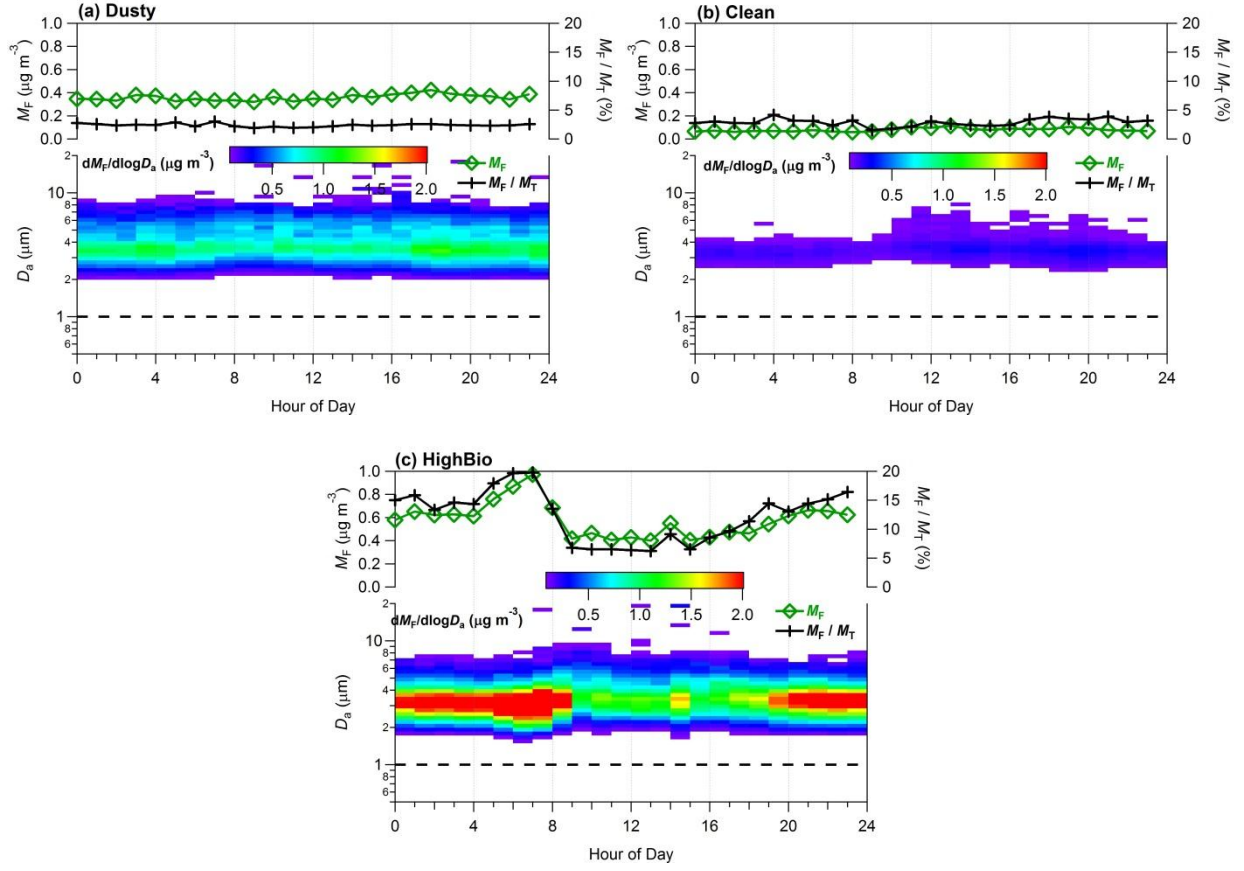


Fig S17: Same and Fig. 13 but representing the FBAP mass (M_F) concentration.

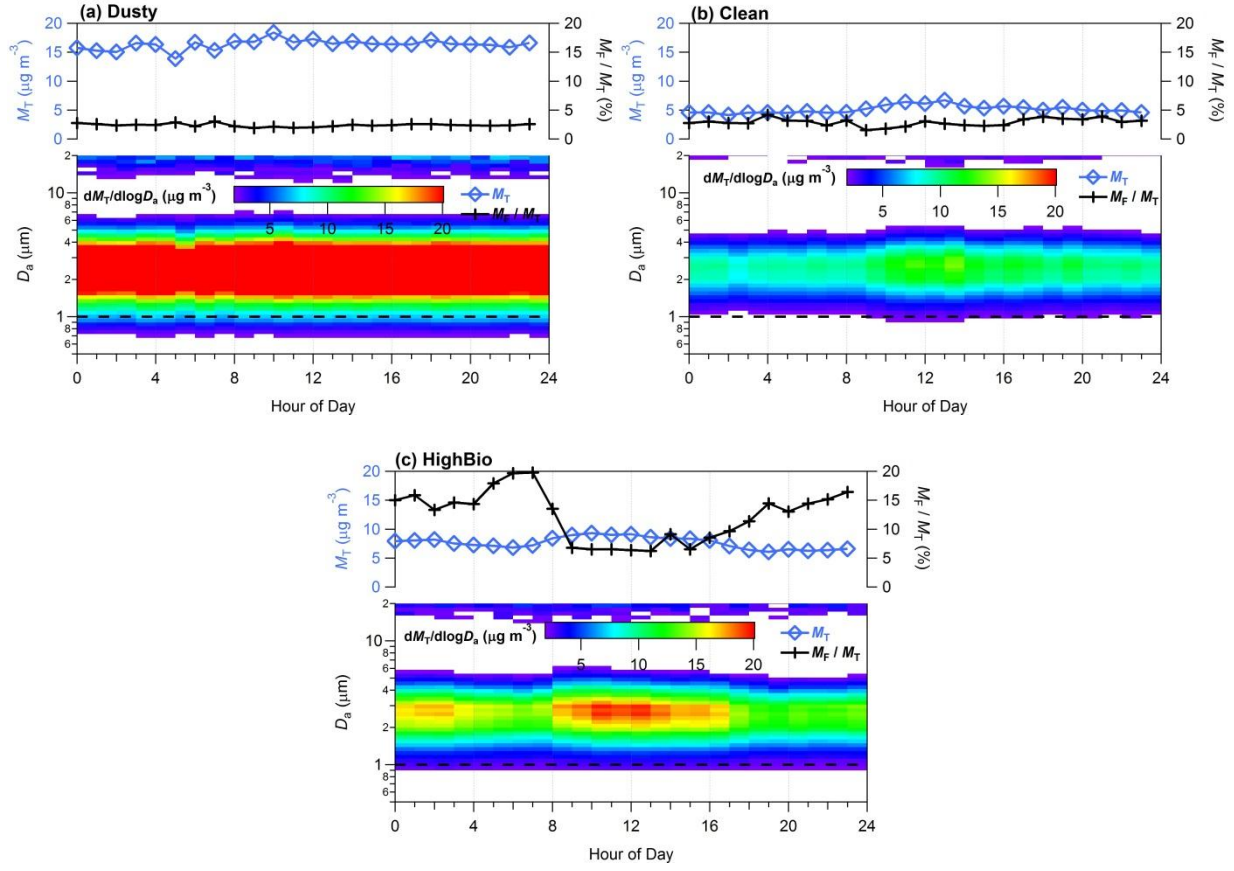


Fig S18: Diurnal cycles of TAP mass concentrations (M_T) and size distributions averaged over each distinct focus periods (hourly median values plotted against the local time of the day).

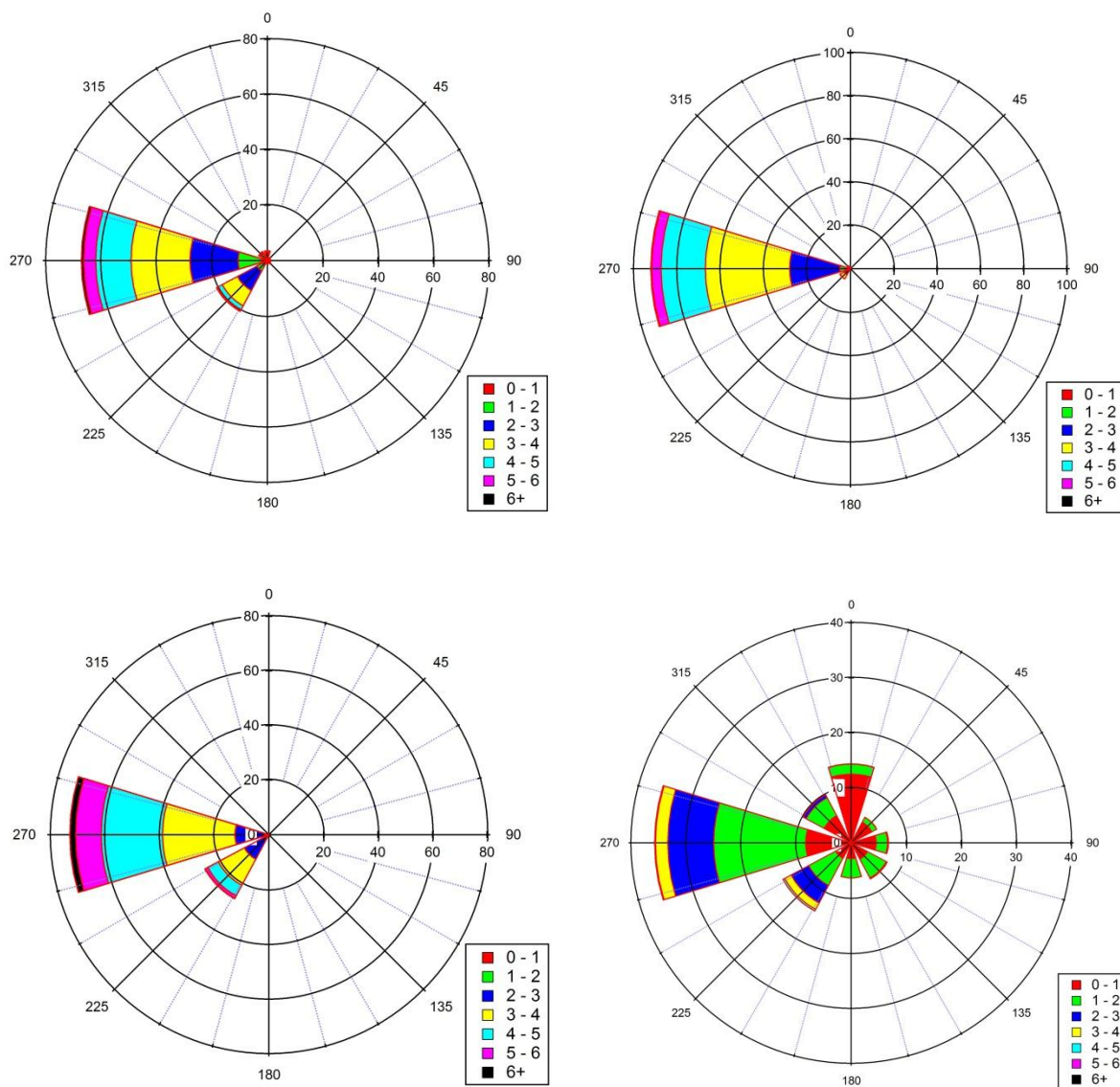


Fig S19: Wind rose diagram scaled over wind speed. (a) entire campaign, (b) dusty, (c) clean, and (d) high bio.

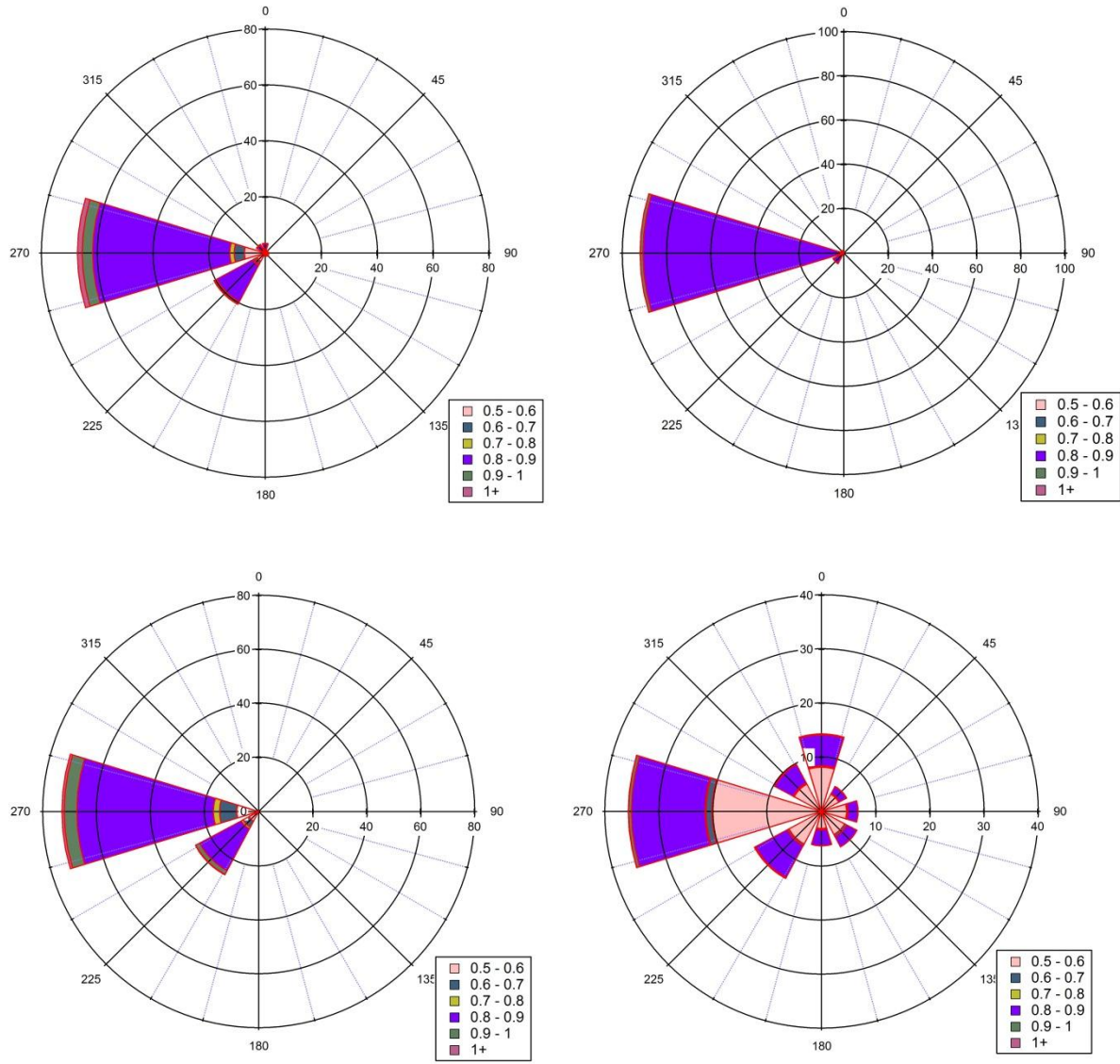


Fig S20: Wind rose diagram scaled by geometric mean diameter ($D_{g,T}$) of $dN_T/d\log D_a$. (a) entire campaign, (b) dusty period, (c) clean period, and (d) high bio period.

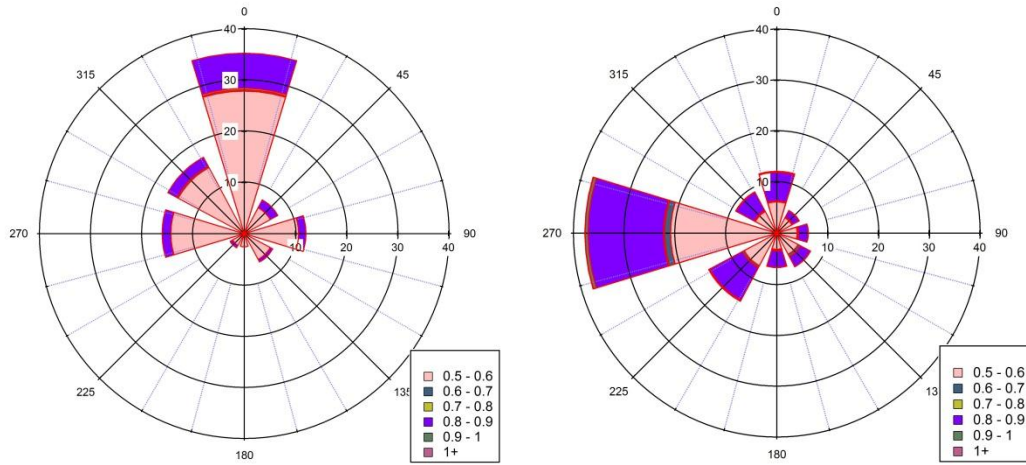


Fig S21: Wind rose diagram scaled by geometric mean diameter ($D_{g,T}$) of $dN_T/d\log D_a$, separated for FBAP number concentration (N_F) range, $N_F > 0.1 \text{ cm}^{-3}$ (a) and $N_F < 0.1 \text{ cm}^{-3}$ (b) observed during high bio period.